Spinal Muscular Atrophy Patient iPSC-Derived Motor Neurons Display Altered Proteomes at Early Stages of Differentiation

Suzy Varderidou-Minasian,* Bert M. Verheijen, Oliver Harschnitz, Sandra Kling, Henk Karst, W. Ludo van der Pol, R. Jeroen Pasterkamp, and Maarten Altelaar*

Read Online

ACCESS | Metrics & More | Article Recommendations | Supporting Information

ABSTRACT: Spinal muscular atrophy (SMA) is an autosomal recessive neurodegenerative disorder characterized by loss of motor neurons (MN) in the spinal cord leading to progressive muscle atrophy and weakness. SMA is caused by mutations in the survival motor neuron 1 (SMN1) gene, resulting in reduced levels of survival motor neuron (SMN) protein. The mechanisms that link SMN deficiency to selective motor neuron dysfunction in SMA remain largely unknown. We present here, for the first time, a comprehensive quantitative TMT-10plex proteomics analysis that covers the development of induced pluripotent stem cell-derived MNs from both healthy individuals and SMA patients. We show that the proteomes of SMA samples segregate from controls already at early stages of neuronal differentiation. The altered proteomic signature in SMA MNs is associated with mRNA splicing, ribonucleoprotein biogenesis, organelle organization, cellular biogenesis, and metabolic processes. We highlight several known SMN-binding partners and evaluate their expression changes during MN differentiation. In addition, we compared our study to human and mouse in vivo proteomic studies revealing distinct and similar signatures. Altogether, our work provides a comprehensive resource of molecular events during early stages of MN differentiation, containing potentially therapeutically interesting protein expression profiles for SMA.
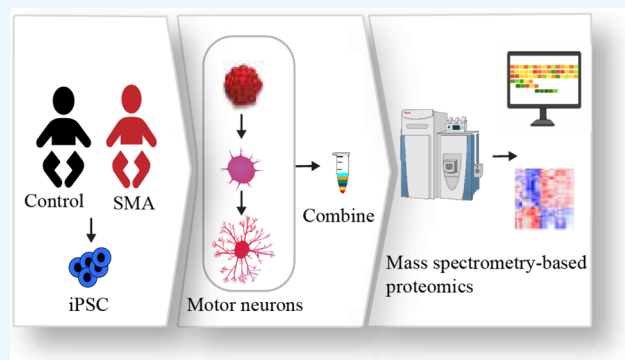
INTRODUCTION

Spinal muscular atrophy (SMA) is an autosomal recessive neuromuscular disease characterized by degeneration of motor neurons (MNs) in the spinal cord, leading to progressive atrophy of muscles and early death in the most severe cases.[1] SMA is the most common inherited cause of infant death, affecting around 1 in 10,000 births.[2] The disease can be roughly subdivided into four main subtypes, depending on the age of onset and the level of acquired motor milestones, ranging from the most severe SMA type I, characterized by neonatal onset, severe weakness, and limited life expectancy, to SMA type IV, with adult onset and mild muscular weakness.[3−5] SMA is caused by reduced levels of survival motor neuron (SMN) protein due to deletions or loss-of-function mutation in the survival motor neuron 1 (SMN1) gene, located on chromosome 5q.[6,7] Importantly, the human genome contains a second gene encoding SMN, that is, SMN2,[8,9] which differs from SMN1 by just a few nucleotides. C → T transition in exon 7 of SMN2 leads to exon skipping, preventing synthesis of stable SMN protein.[1,10,11] Consequently, SMN2 only produces low levels of full-length SMN protein and cannot fully compensate for loss of SMN1. Notably, SMN2 shows copy number variations in patients and the SMN2 copy number is an important determinant of disease severity.[10,12−14]

The SMN protein is ubiquitously expressed and has been studied in great detail for its role in the assembly of small nuclear ribonucleoproteins, which are important for the formation of spliceosomes that carry out pre-mRNA splicing in the nucleus.[15,16] Remarkably, reduced levels of the ubiquitously expressed SMN protein predominantly affect lower MNs in SMA.[17] To date, it remains unclear why SMA pathology has been largely restricted to this specific cell population.[18,19] Several mechanisms have been suggested though, such as cellular functions of SMN that are specific to MNs or increased sensitivity of MNs to reduced levels of SMN, for example, due to the length of their axons and unique interactions with skeletal muscles. Cell type-specific splicing abnormalities caused by SMN deficiency could contribute to the selectivity of SMA pathogenesis, although such splicing defects appear to be mostly relevant during later stages of the disease.[20,21] Additionally, it is known that SMN is expressed in
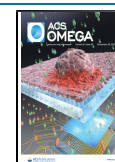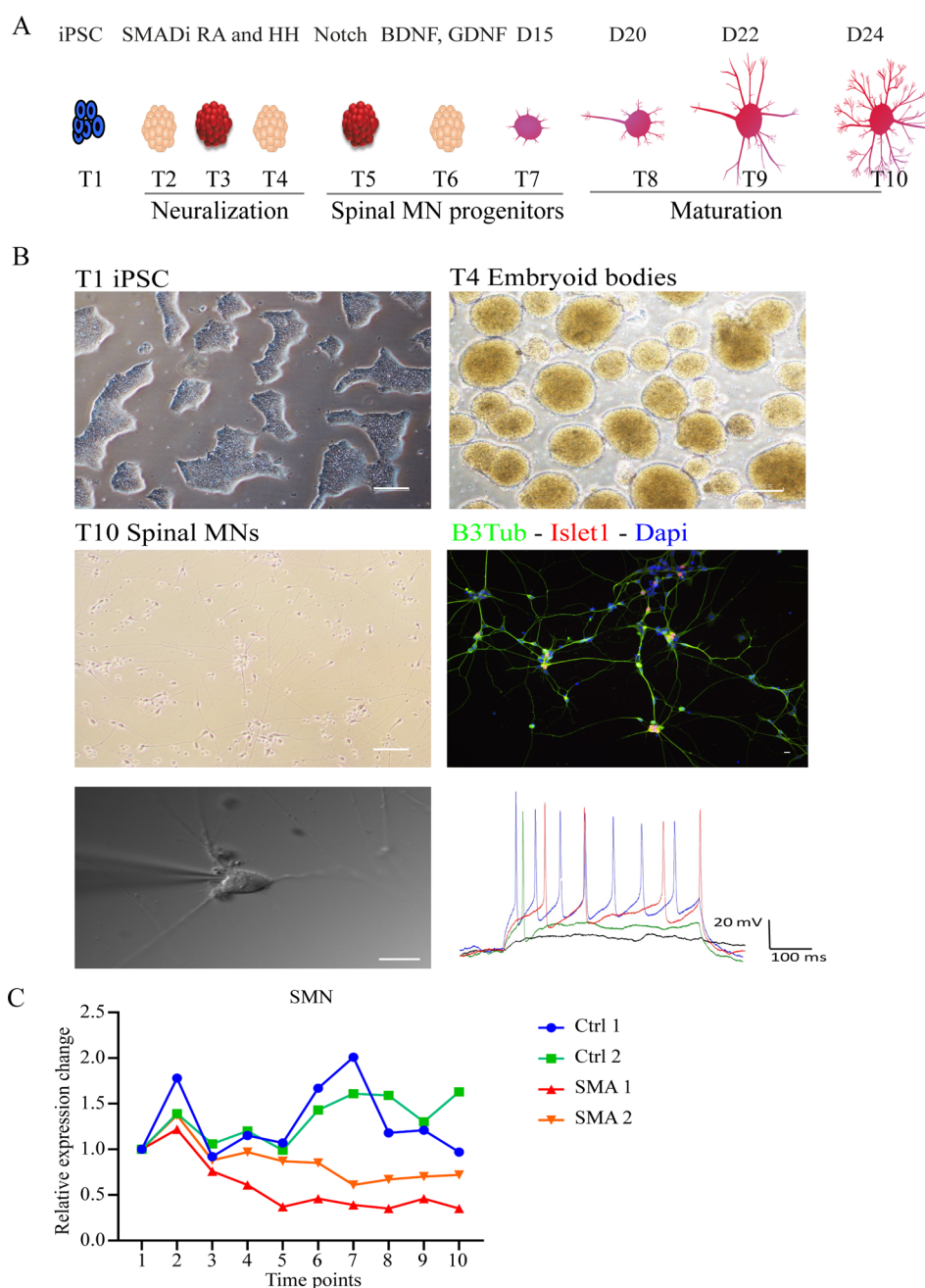
Figure 1. (A) Experimental workflow of iPSC differentiation toward MNs. Cells were treated with SMAD inhibitors, smoothened agonist, retinoic acid, DAPT, BDNF, and GDNF. At indicated time points, cells were lysed for proteomic analysis. (B). MN differentiation at indicated time points. Phase contrast image of iPSCs at T1, EBs at T4, and MNs at T10. Scale bar, 100 μm. MNs at T10 were immunostained with a neuronal marker (B3Tubulin), a motor neuron marker (Islet1), and a nuclear marker (DAPI). Patched MNs and example of traces showing action potential generation. Scale bars: T1 is 100 μm; T4 is 200 μm; and T10 is 40 μm. Patched MNs' scale bar is 25 μm. (C) SMN protein expression extracted from the proteomic data showing changes during spinal MN differentiation of healthy controls and SMA patient-derived material.

growth cones of MNs during neuronal differentiation and that it modulates axon growth and interacts with β-actin mRNA, suggesting that SMN functions in the development of MNs by allowing normal axon growth and transport of RNA.[22−24] SMN is also important to skeletal muscle fibers.[22,25,26] Spectacular advances have recently been made in SMA therapy, in particular using gene therapy for replacement of *SMN1* and antisense oligonucleotides or small molecules that manipulate splicing of *SMN2*, which have dramatically changed the natural history of the disease.[27] Despite these changes in the treatment landscape, there is a general lack of under-

standing of how molecular pathways are acting downstream of SMN to cause SMA. Furthermore, SMA is often studied at late stages in pathogenesis, but it is becoming increasingly apparent that abnormal (neuro) development is a critical component of SMA pathology and that early therapeutic intervention will be necessary.[28] Efforts have been made to identify biomarkers for SMA, which resulted in a number of molecular biomarkers such as the SMN2 copy number, SMN mRNA and protein levels, neurofilament proteins' plasma protein analytes, creatine kinase, creatinine, and various electrophysiology and imaging measures.[29] The study of early neurodevelopmental processes
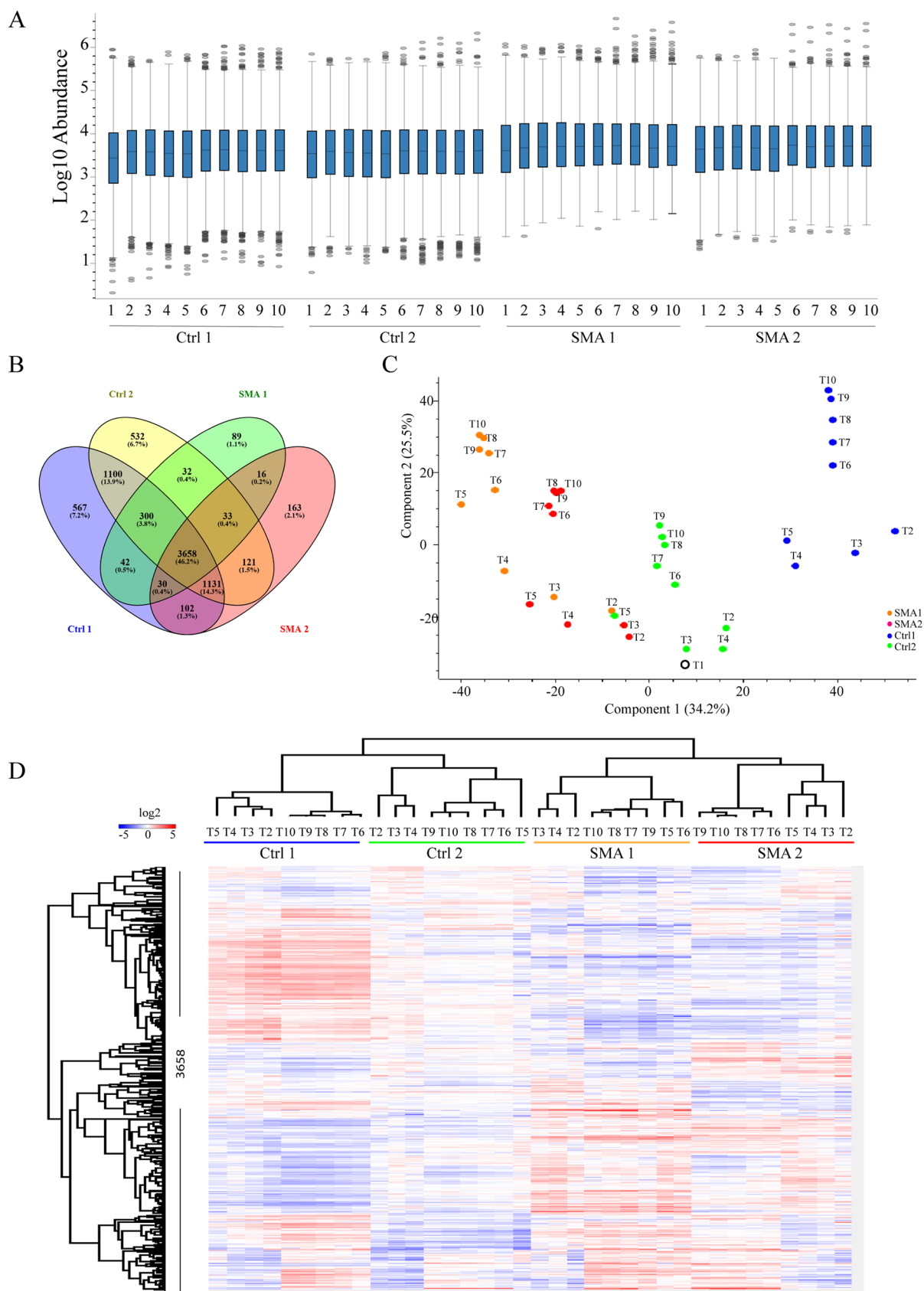
Figure 2. (A) Box plots of $\log_2$ transformed data normalized on protein peak areas of each individual replicate. (B) Venn diagram showing the proteins identified in each biological replicate and time points. (C) PCA of the proteome at all time points during differentiation of healthy controls and SMA patient-derived material segregates component 1 into healthy and disease and component 2 into time points. (D) Hierarchical clustering of each sample and time points.
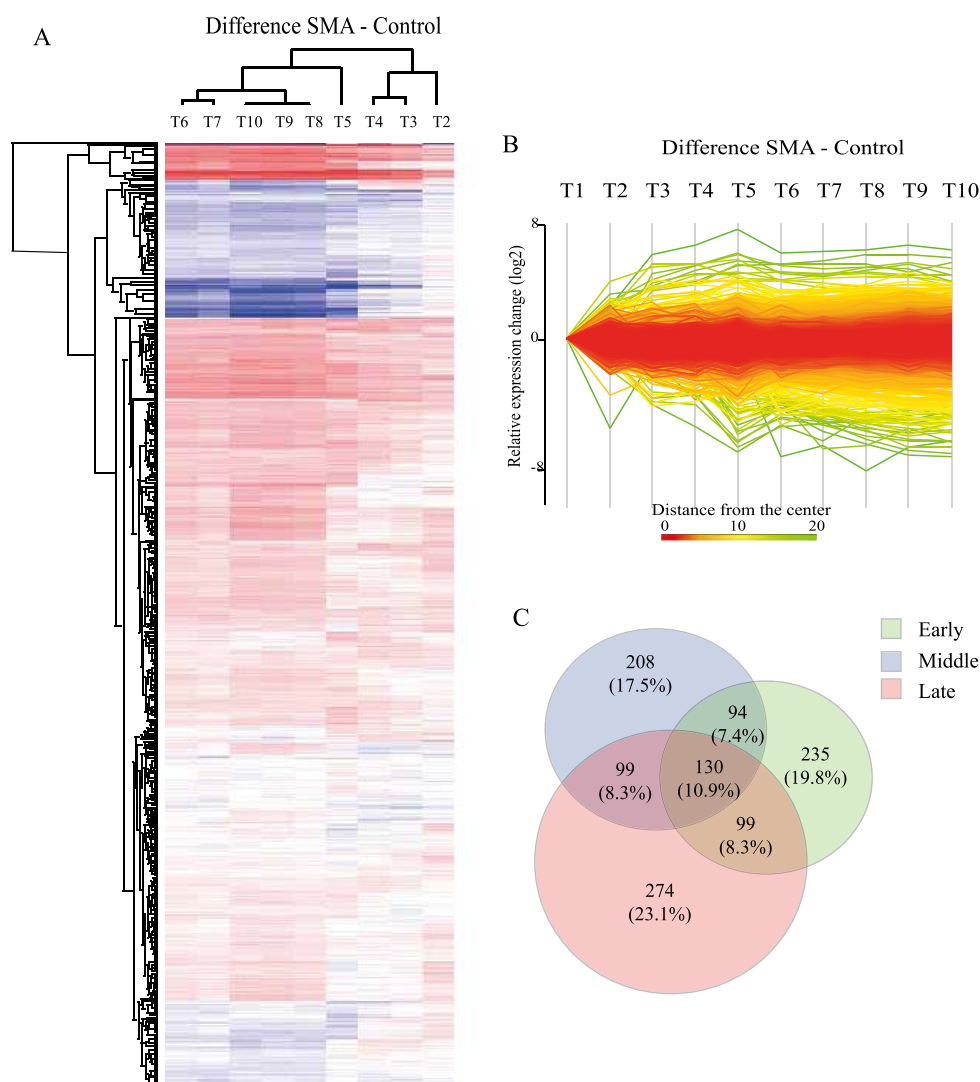
Figure 3. (A) Heat map of the significantly regulated proteins [*p* value cutoff (0.1) and fold change ≥1.3] at all time points. (B) Profile plot of the significant proteins at indicated time points. (C) Venn diagram showing the overlay of the significant proteins in the three periods during MN differentiation.

in disorders such as SMA has become feasible through the generation of induced pluripotent stem cells (iPSCs), derived from, for example, human fibroblasts, which hold great promise in the investigation of neurological diseases.[30] This technology has made it possible to generate human neurons, including MNs, to study disease mechanisms and potentially identify (better) treatments for human disorders. iPSCs-MNs have also been used to recapitulate SMA pathology.[31−36] While SMA patient iPSC-derived MNs have been compared to healthy MNs in previous studies, the precise changes occurring during MN differentiation in SMA remain elusive. Analyzing proteome changes during MN development in a genetic SMA background can be a means to improve our understanding of SMA in an unbiased manner and unravel SMA-associated molecular pathways. Doing so will require large-scale mass spectrometry approaches with quantitative assessment. Such proteomics approaches have recently been used to study normal neuronal development and neurodevelopmental disease in detail.[37−39]

The aim of our study was to evaluate specific proteome changes that occur during MN differentiation of SMA patient and healthy control-derived iPSCs. We quantitatively moni-tored the MN proteome at 10 time points during differentiation [using tandem mass tag (TMT)-10plex], revealing early changes in molecular processes in SMA. Furthermore, we quantitatively monitored known SMN-binding partners that function in RNA splicing and visualized their expression levels during MN differentiation.

■ RESULTS

Generation of iPSCs from SMA and Control Samples That Differentiate toward Spinal Motor Neurons. SMA (SMA1 and SMA2) and control (Ctrl1 and Ctrl2) iPSC lines were generated from skin fibroblasts using lentiviral trans-duction of four transcription factors OCT4, KLF4, SOX2, and c-MYC, as previously described (see Table S1 for clinical history and origin) and characterized using a range of standardized pluripotency assays (Figure S1A).[40,41] Resulting iPSCs were able to differentiate into different cell lineages (mesoderm, endoderm, and ectoderm), and karyotype analysis showed no chromosomal aberrations (Figures S1B and S2). Using a slightly modified version of the procedure described by Maury et al.[42] iPSCs were differentiated into lower spinal
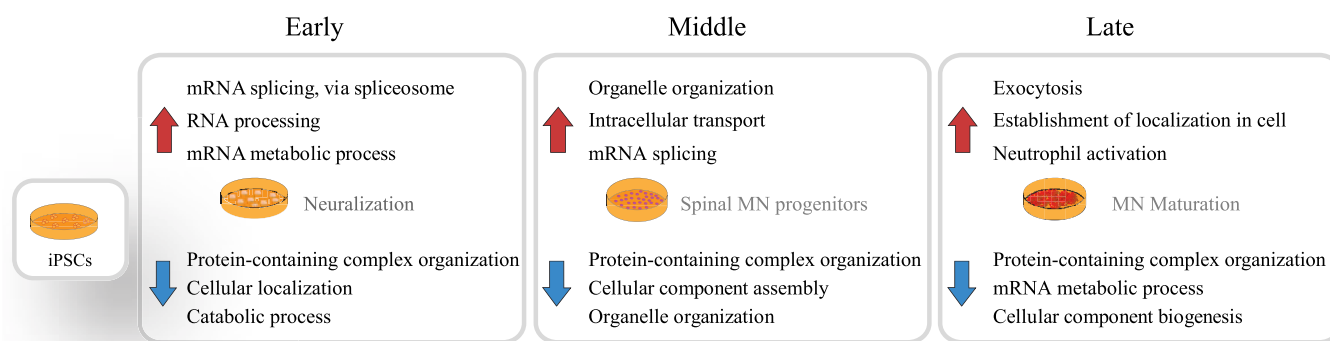
Figure 4. Summary of biological processes during MN differentiation in SMA. Biological processes that are either upregulated or downregulated in SMA in the course of spinal MN differentiation. The differentiation timeline is represented as neuralization (early), spinal MN progenitors (middle), and MN maturation (late).

MNs. Briefly, embryoid bodies (EBs) were induced to promote differentiation of iPSCs. For neuralization, dual-SMAD signaling was inhibited for 4 days, followed by the addition of caudo-ventralizing factors containing retinoic acid and a sonic hedgehog agonist.[43] On day 15, EBs were dissociated into single cells and underwent further maturation for another 9 days. At this point, MNs were positive for the neuronal marker βIII-tubulin (>80%) and motor neuron marker ISL1 (~40%) (Figure 1A,B). Electrophysiological recordings of MNs further showed that MNs were able to fire repetitive action potentials. During MN differentiation, levels of SMN were reduced in SMA, compared to healthy controls, with SMA1-line showing the largest reduction (Figure 1C). Interestingly, the difference between SMA and controls increased from T5 onwards, at which point neurite outgrowth and maturation occur. Together, these data demonstrate that both SMA and control iPSCs can differentiate toward lower MNs that can be used as an in vitro model to study SMA.

SMA iPSC Differentiation toward MNs Shows Altered Proteomic Signature. To resolve proteome changes in SMA during MN differentiation, samples from 10 distinct time points within the differentiation timeline were subjected to in-depth quantitative proteome analysis. Samples at indicated time points were digested into peptides, labeled with TMT-10plex, fractionated by high-pH fractionation, and analyzed using liquid chromatography coupled to high-resolution mass spectrometry (LC−MS/MS) analysis. We identified 8049 proteins with a false discovery of 1% and quantified 3658 proteins across all time points in all biological replicates. Furthermore, the ratio distribution was examined between replicates and time points (Figure 2A,B). This approach allowed us to identify (and subsequently quantify) low abundant components of the cellular proteome, including the SMN protein and components of the SMN core complex,[44] which will be discussed in more detail. For our quantitative data analysis, we normalized all values of each time point to the reference value of iPSC protein expression before initiation of differentiation (T1). This allowed us to quantitatively compare the protein changes during MN differentiation between the different samples. All data throughout the study reflect a log$_2$ transformed ratio change relative to T1 for each biological replicate.

To get an overview of the whole-proteome changes between SMA and control samples, we performed principal component analysis (PCA) at all time points (Figure 2C). This revealed that SMA samples were largely segregated from controls in component 1 (accounts for 34.2% of variability), demonstrating proteome alterations between SMA and control cell lines already at early stages during neuronal differentiation. Component 2 segregates the time points during MN differentiation (with 22.5% of variability). To get an overview of the profiles of all quantified proteins, we plotted the expression values of the samples at each time point and visualized these in a heatmap (Figure 2D). By unsupervised hierarchical clustering of the 3628 proteins, SMA samples formed a distinct cluster compared to the controls. Remarkably, within each biological replicate, two clusters are formed separating the time points in two groups.

Proteome Alterations at Different Stages of MN Differentiation. All identified proteins were filtered based on identification of proteins by three or more unique peptides. This decreased the number of proteins from 8049 to 6063 proteins. To further investigate the changes in the proteome of SMA- versus control MNs during development, we compared the proteome of the samples at each time point separately. In Figure S3, we show volcano plots comparing all time points relative to T1. For additional stringency, a threshold for significantly regulated proteins is chosen for a p value cut off (0.1) and a fold change ≥1.3. This resulted in 1267 significantly regulated proteins derived from all time points together (Table S2). To gain insights into how the differentially expressed proteins in SMA behave across time points, we further averaged the log$_2$ values of SMA and extracted with control for each time point. The difference between SMA and control at each time point is shown in a heat map (Figure 3A). Hierarchical clustering of the time points segregates them into early time points (T2, T3, and T4), middle (T5) (T6 and T7), and late (T8, T9, and T10). During these time points, the iPSCs differentiate toward MNs based on three periods: neuralization (T2, T3, and T4), spinal motor neuron progenitors (T5, T6, and T7), and maturation (T8, T9, and T10). We compared the difference value of these significantly expressed proteins from all time points and noticed that the difference between SMA and control is increasing over time (Figure 3B). Within the indicated proteins, we considered the time points T2, T3, and T4 as *early*, T5, T6, and T7 as *middle*, and T8, T9, and T10 as *late* referring to their differentiation periods. We compared the differentially expressed proteins in SMA in the three timelines (early, middle, and late) in a Venn diagram and showed the
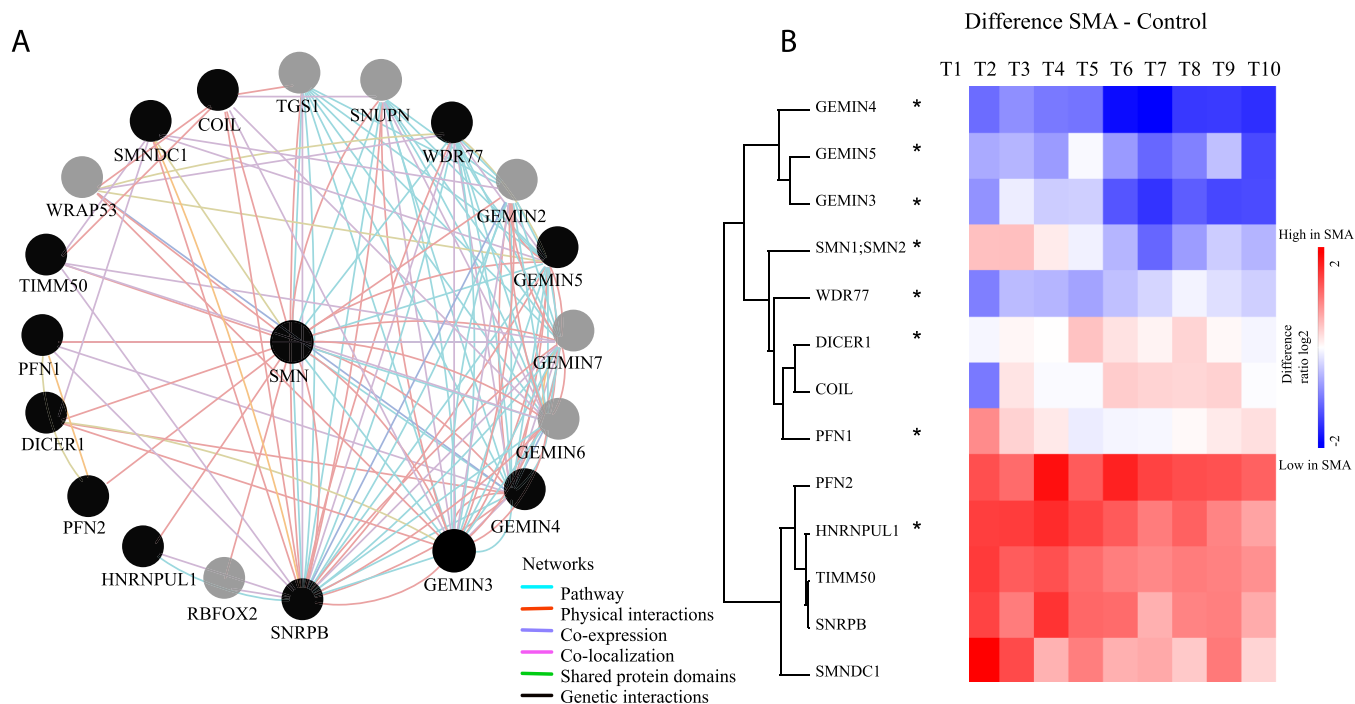
Figure 5. (A) Network analysis of SMN-binding partners derived from Cytoscape (Genemania plugin). The gray color indicates that the protein is not identified and the black color indicates that the protein is identified by mass spectrometry measurements. (B) Heat map showing the difference value between SMA and control for each protein. The red color indicates higher expression in SMA compared to controls and blue indicates a lower expression level in SMA. Asterisk indicates that the protein was significantly different (FDR ≤ 0.05) in iPSC-derived spinal MNs of SMA patients.

overlap over time (Figure 3C). Approximately 10% of the proteins is differentially expressed at all time points and the large majority (23.1%) is differentially expressed during maturation (late). The differentially expressed proteins in SMA were examined using Gene Ontology (GO) enrichment analysis in terms of potential biological processes.[45] Processes such as "mRNA splicing", "organelle organization", "exocytosis", and "neutrophil activation" were upregulated in SMA (Table S3).

Processes related to "protein-containing complex organization", "cellular component biogenesis", and "catabolic process" were downregulated in SMA (Figure 4). Dysregulation of mRNA splicing is well described as a hallmark in SMA disease, adding further validity to this developmental model's ability to capture elements of the patient conditions.[18] Furthermore, previous studies have shown altered ER to Golgi vesicle transport in relation to SMA, which in this case reflects similar findings in the iPSC-derived MNs.[46,47] These results seem to indicate that the SMA genetic background has a substantial impact on the development of MNs and that alterations in cellular processes associated with late-stage SMA already manifest themselves at early stages of the disease. Conversely, previous studies have shown dysregulation of neuronal development at later stages of mature MNs,[44] but not during maturation. In addition, the differentially expressed proteins in SMA were examined in terms of cellular compartment, molecular function, and kegg pathways. Downregulated proteins in the early, middle, as well as in the late time points were localized in the nucleus, while upregulated proteins were localized in the nucleus and in the extracellular vesicles. The molecular functions of the downregulated proteins as well as the upregulated proteins are categorized into "RNA binding" and "nucleotide binding". Furthermore, proteins downregu-

lated in SMA are categorized into "RNA transport", "DNA replication", and "mismatch repair" in the kegg pathway. Proteins upregulated in SMA are categorized into "spliceosome", "lysosome", and "Huntington disease".

SMN-Binding Partners and Splicing. To further investigate the mechanism by which SMN mutations influence SMA, we examined known SMN interaction partners (Cytoscape, Genemania plugin) along MN differentiation. By drawing a protein interaction network around SMN as the input, we identified 20 connected binding partners having a role in RNA splicing of which 13 were identified in our proteomics measurements during MN differentiation (Figure 5A). To get an overview of the altered expression profiles of these 13 proteins during MN development in SMA, we determined the difference in intensity values observed in SMA versus control iPSC lines, which we visualized in a heatmap (Figure 5B). Of these, SMN, GEMIN3, GEMIN4, GEMIN5, WDR77, DICER1, PFN1, and HNRNPUL1 proteins were significantly enriched [false discovery rate (FDR) ≤ 0.05] during MN maturation. Interestingly, the interaction between Gemins 2−8, Unr-interacting protein and SMN, is the determining factor for SMA. SMN and Gemins form a complex, which constitutes the building blocks of spliceosomes. Reduced levels of Gemins lead to development of motor deficits that are similar to those observed on attenuation of SMN in *Drosophila*.[48] This might be interesting to consider that inadequate levels of any one member rather than SMN only is sufficient to arrest the SMN complex and the normal motor neuron development. WDR77 was previously shown to interact with SMN and Gemins as well, indicating its involvement in SMA.[49] Dicer1 is a ribonuclease that functions in nucleic acid binding and it is required to cleave dsRNA and pre-miRNA into siRNA and miRNA. Transgenic mice

harboring loss of Dicer function showed abnormal motor neuron development that resembled SMA.[50] This confirmed the relevance of miRNAs in the regulation and function of MN. HNRNPUL1 is an RNA-binding protein involved in mRNA splicing. Its association with SMA is unclear; however, several other HNRNP members were identified to interact with SMN in MNs.[51,52] Finally, mutations in the PFN1 gene have been shown to cause another motor neuron disease, amyotrophic lateral sclerosis (ALS), and result in MNs having shorter axons and smaller growth cones,[53] but its association with SMA has not yet been studied.

Splicing is an essential process, where introns are removed and exons are joined together to generate mRNA. An altered splicing pattern is a well described hallmark in SMA, therefore, we captured all proteins associated with splicing from the reactome pathway and visualized their expression during MN differentiation (Figure 6). The majority of these proteins are downregulated in SMA compared to healthy controls. Interestingly, the altered expression pattern of these proteins was present already at early stages of MN differentiation, suggesting that splicing dysregulation may be an early hallmark of SMA. Overall, we show a specific regulation of functionally distinct subgroups of the proteome around SMN-binding partners and splicing associated proteins at specific stages during MN differentiation.

Comparison to Mouse and Human In Vivo Proteome Data. In order to evaluate how well our human in-vitro-derived proteomic study resembles other model systems in SMA and to identify a common protein signature in SMA, we compared our results to human and mouse in vivo models of SMA. We screened in the literature study containing mass spectrometry-based proteomic data on human and mouse model of SMA to provide an unbiased evaluation of potential biomarkers. To identify publicly available proteomic datasets of SMA, PubMed was searched using the following search string: SMA, human or mouse, and mass spectrometry or proteomics. This search yielded 42 matches for human and 16 matches for mouse models. We evaluated the studies individually to identify studies containing raw data comparing SMA with controls. From this, datasets from three studies were suitable for the comparison with our data. Motyl et al. compared the brains of a prenatal mouse model of SMA with control samples to identify presymptomatic developmental abnormalities.[54] This analysis revealed 7231 proteins identified in SMA and control mouse brains. In addition, Finkel et al. took blood specimens from SMA and healthy individuals for proteomic analysis and identified 701 proteins in plasma across 127 samples.[55] As last, we used the dataset from Fuller et al., where they generated iPSC-derived MN from type I SMA and healthy controls and 2125 proteins were identified across the samples.[56] In Figure 7, we show a Venn diagram of the proteomic comparison across these studies. Our data resemble most those of the in vitro study of Fuller, both derived from iPSC-derived MNs. We detected 1891 proteins out of 2125 in total in our dataset. Out of these, 115 proteins were significantly regulated in both datasets (we considered proteins significant with a ratio of 20%-fold change relative to controls in the study of Fuller et al.) (Table S5). When we compared the upregulated and downregulated proteins from both datasets, we identified several proteins having opposite directions. 35 proteins were significantly downregulated in our dataset while being significantly upregulated in the in vitro study of Fuller et al. In addition, 21 proteins were significantly
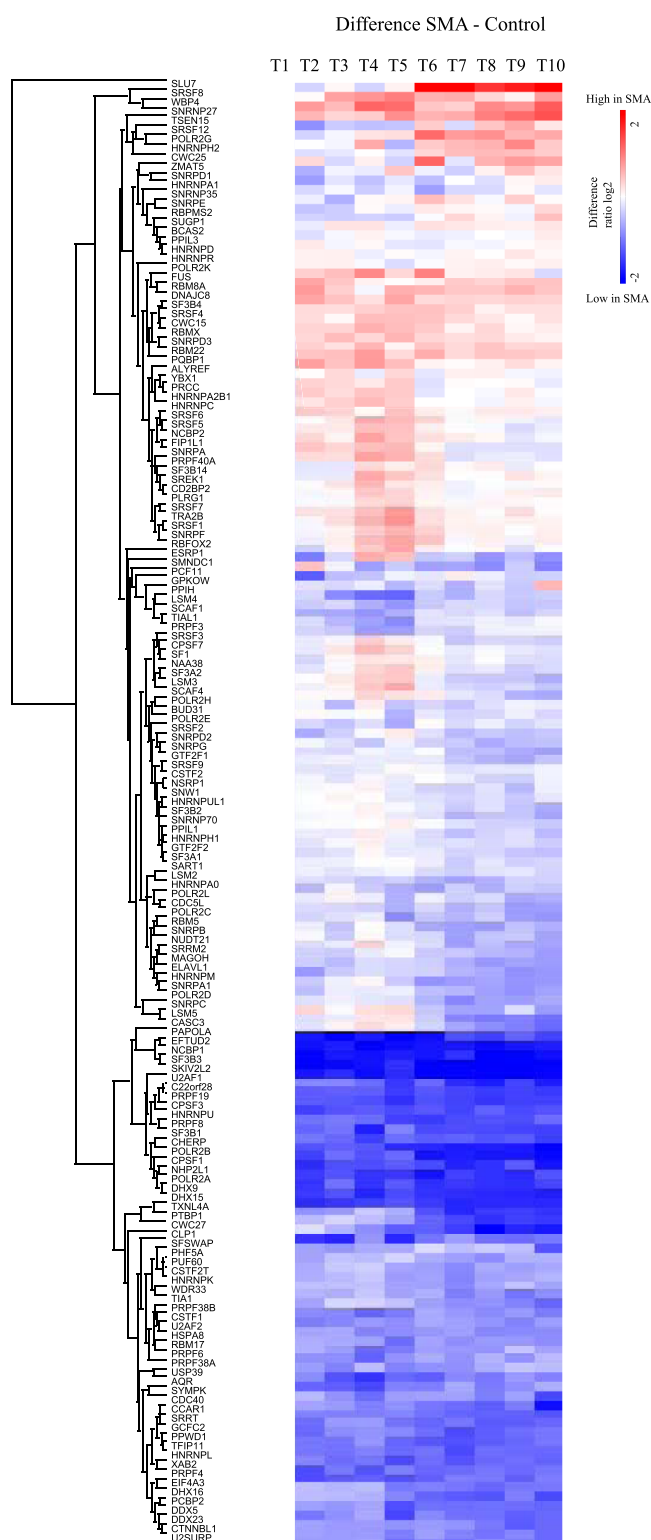

Figure 6. Heatmap of protein expression changes associated with splicing.

upregulated in our study and downregulated in the in vitro study. Out of these, we identified 59 proteins being significantly regulated in both studies and having the same direction. They play a role in protein localization to endoplasmic reticulum and a translational response to unfolded protein. We then compared our study to the human plasma proteomic study of Finkel et al. and identified
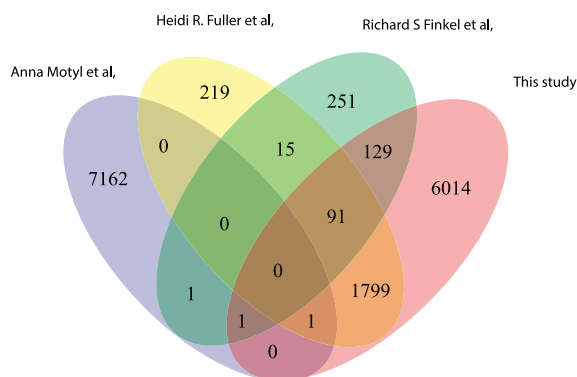
Figure 7. Venn diagram showing the number of identified proteins and the overlap in the four studies.

92 proteins in both datasets. Out of these, only NCAM and RPS27A were significantly regulated in both studies. Finally, our study resembles least with the in vivo mouse study of Motyl et al., where only two proteins (FAM120A and C3) were identified in both datasets, not being significantly regulated. Overall, these proteomic comparisons provided here are a useful resource for exploring the molecular consequences of SMN reduction and for the identification of novel biomarkers and therapeutic targets for SMA.

■ DISCUSSION

Because reduced levels of SMN protein in MNs cause SMA, major efforts are ongoing in both academia and industry to discover and improve SMN-elevating therapeutics to treat SMA.[57] However, the exact mechanisms that are responsible for SMA remain poorly understood. Improved insights into the mechanisms that underlie SMA are important because they may inform treatment strategies (e.g., to delineate the therapeutic window of opportunity in patients) and result in the identification of new therapeutic targets. Also, efforts have been made to identify biomarkers for SMA, such as SMN mRNA and protein levels, neurofilament proteins plasma protein analytes, creatine kinase, creatinine, and various electrophysiology and imaging measures.[29] Discovery of new biomarkers that are linked to SMA disease processes will be of interest for future studies involving longitudinal follow-up of patients, for example, during treatment. Here, we describe the use of human iPSC technology and mass spectrometry to quantitatively study proteome changes during the entire timeline of MN differentiation in SMA patients and control cells. Evaluation of our quantitative proteomics data indicated altered protein expression already occurring during neuralization and in spinal MN progenitors and revealed the largest differences in protein expression profiles between the SMA patients and control cells in mature MNs. In particular, proteins associated with intracellular transport, localization, and biogenesis were downregulated, consistent with previous studies describing defects in late stages of MNs.[18,47,58−61] Here, we provide evidence of altered proteomic changes in these pathways at early developmental stages. These data serve as a valuable resource of potential targets for early treatment in SMA to reduce the progression of symptoms.

We specifically examined SMN protein levels during SMA and control iPSC-MN differentiation. We noted that differences in SMN levels between SMA and controls started to increase from T5−T7 onwards, when dendrites and axons start

to develop and mature. This may suggest that differences in SMN levels in SMA compared to controls are restricted to the later stages of MN differentiation. While a previous study reported such delayed neurite outgrowth, and a decreased number of neurites in iPSC-derived MNs from SMA patients, the difference in SMN was not obvious, due to a low percentage of MNs.[62] This may suggest that MN vulnerability and neuritic abnormalities at these stages could thus be linked to lower levels of SMN. Decreased SMN levels in mouse nervous tissues were previously observed only in SMA mice during maturation, whereas SMN levels in control mice remained relatively stable.[63] These results may indicate that the level of SMN is important during MN maturation. Because there is selective degeneration of lower MNs in SMA patients with reduced SMN protein expression, and given that SMN has a neuron-specific role in mRNA processing, it is not surprising that the difference in protein expression between SMA and healthy controls is increased during the generation of MNs.[64,65] Although the difference of the SMN level between controls and SMA is low at the early stages, this increases at the late stages. In addition, the majority of the significantly regulated proteins were divergent between SMA and controls at later stages of MN differentiation.

When we analyzed the proteome of SMA patients and healthy controls during MN development, we found that the proteome of SMA segregates from healthy controls at early time points and that the differences between SMA and healthy cells increase even more at later time points of MN differentiation. Proteins downregulated in SMA are involved in ribonucleoprotein complex biogenesis, DNA metabolic processes, and intracellular transport. Proteins upregulated in SMA are involved in mRNA splicing, organelle and mitochondrion organization, protein folding, and neutrophil-mediated immunity. Moreover, these processes were more strongly enriched at later stages of development, during MN maturation. The early altered proteomes identified in our in vitro study are in line with a recent in vivo study showing presymptomatic changes in a prenatal mouse model of SMA.[54] Here, SMA mouse embryos were smaller than their controls, and at the protein level the cytoskeleton and RhoA/ROCK signaling pathways were affected. In line with this, we identified altered cytoskeletal proteins at middle and late stages of differentiation. This suggests a developmental delay at the protein level that can contribute to SMA pathology.

Efforts to improve SMA therapy can potentially benefit from combinatorial strategies next to SMN-elevating therapeutics and could benefit from exploring novel targets at early stages of disease.[57] In our dataset, we, therefore, investigated the protein expression patterns of known SMN-binding partners during MN differentiation. This identified several SMN-binding partners that show significant alterations in SMA and are potential useful candidates to consider further. Especially, members of the Gemins, which are a constituent in the spliceosome complex, would be an interesting candidate for a further study in relation to SMA.[66] Furthermore, the expression behavior of the here highlighted proteins should be further studied in the light of the disease-ameliorating effect of increasing SMN levels, using compounds such as MLN4924 and splicing modulator C3, which were previously used to increase SMN levels in SMA,.[35,67−69] This combination may prioritize protein candidates for targeting in combinatorial therapy strategies.

An interesting result was the altered expression of HSPB1, which was also found to be differentially expressed in SMA iPSC-MN in a previous study.[34] HSPB1 is a small heat shock protein involved in cell survival, as well as many other processes. Mutations in HSPB1 have been found in distal hereditary motor neuropathies and axonal Charcot Marie tooth type 2, hinting at an important role for HSPB1 in MN and, potentially, shared molecular mechanisms between SMA and these other disorders.[70,71]

Despite the fact that SMA is considered to mainly affect spinal MNs, recent studies have suggested that other neuronal tissues might be affected as well, including brain structures such as the hippocampus.[72,73] Therefore, studying different neuronal subtypes will be essential to analyze the development and neuronal maturation phenotypes found in SMA. 3D organoid models could provide a useful platform for such studies. In addition, human iPSC-derived MNs were recently cocultured with other cells, such as endothelial cells and muscle fibers, on microfluidic "organ-on-chip" platforms to model cellular interactions involved in MN diseases,[74,75] and SMA iPSC-derived spinal MNs grown on these devices could better mimic SMA pathology and advance our understanding of disease progression.

A limitation of our study is the low number of samples that has been analyzed. We used two SMA-derived samples and two healthy control samples. Even though this approach allowed us to study early alterations in SMA, the introduction of isogenic controls (e.g., CRISPR-induced or -corrected cell lines) should be considered in future studies to study the exact contribution of SMN, as well as experiments that validate target proteins identified in this study.

In conclusion, iPSCs generated from SMA patients were differentiated into spinal MNs in culture to examine proteins with altered neurodevelopmental signatures. This revealed that SMA MN proteomes are different from control MN proteomes at early stages of MN differentiation. Efforts to improve SMA therapy can potentially benefit from combinatorial strategies that combine SMN-elevating drugs with therapies that target specific mechanisms at early stages of the disease. The findings described here can be used to identify proteins that are changed before the onset of disease symptoms and could be used to screen for a novel biomarker and/or therapeutic candidates.

■ MATERIALS AND METHODS

Ethics Statement. Skin fibroblasts were obtained from 2 SMA type I patients and 2 healthy controls and stored in liquid nitrogen. A summary of the patients and control lines can be found in Table S1. Control fibroblasts were provided by Dr. Vivi M. Heine (VU University, Amsterdam, the Netherlands). Both SMA patients were type I, defined by the presence of 2 copies of SMN2. All protocols in this study were carried out in accordance with guidelines approved by the Medical Ethical Committee of the University Medical Center Utrecht.

Generation of iPSCs. Primary human fibroblasts were maintained in mouse embryonic fibroblast (MEF) containing Dulbecco's modified Eagle's medium (DMEM) glutamax (Life Technologies), supplemented with 10% fetal bovine serum (Sigma-Aldrich) and 1% penicillin/streptomycin (Life Technologies). Viral transduction was performed as described previously.[76] Briefly, a lentiviral vector expressing OCT4, KLF4, SOX2, c-MYC, and a mixture containing MEF medium and 4 mg/mL hexadimethrine bromide (Sigma) was used.

Cells were incubated for 24 h in this mixture, followed by MEF medium for 5 days. Hereafter, cells were transferred to irradiated MEFs in human embryonic stem cell (huES) medium containing DMEM-F12 (Life Technologies), knock-out serum replacement (Life Technologies), penicillin/streptomycin, L-glutamine (Life Technologies), non-essential amino acids (Life Technologies), β-mercaptoethanol (Merck Millipore), and 20 ng/mL recombinant human fibroblast growth factor-basic (bFGF; Life Technologies). Potential iPSC colonies were selected on the basis of their embryonic stem cell-like morphology. Feeder-free iPSCs were cultured on Geltrex-coated dishes (Life Technologies) in mTeSR1 medium (Stem Cell Technologies) and passaged enzymatically with Accutase (Innovative Life Technologies). All cell lines were tested for mycoplasma contamination every other week.

Karyotyping. All iPSC lines were incubated for 30 min at 37 °C in Colcemid (100 ng/mL; Life Technologies) and dissociated with trypsin (TrypLE) for 10 min. Following this, cells were washed with phosphate buffered saline (PBS) and incubated for 30 min in 5 mL hypotonic solution (1 g potassium chloride and 1 g sodium citrate in 400 mL H_2O). This was followed by centrifugation for 3 min at 1500 rpm and fixation for 5 min at room temperature with methanol/acetic, 3:1. Cells were then resuspended and subjected for G-band karyotyping.

Motor Neuron Differentiation. Motor neuron differentiation was performed using a slightly modified version of a previously described protocol.[42] Briefly, on day 0, iPSCs were gently lifted by Accutase treatment for 5 min at 37 °C and resuspended in differentiation medium [DMEM F-12, Neurobasal v/v, N_2 supplement (Life Technologies)], B27 without vitamin A (Life Technologies), Pen−strep 1%, ascorbic acid 0.5 μM (Sigma-Aldrich), and 5 μM Y27632 (STemGent). EBs were formed through a standardized microwell assay by seeding at a density of 150 cells/microwell in differentiation medium.[77] For neuralization, dual-SMAD signaling was inhibited for 4 days with 3 μM Chir-99021 (Tocris), 0.2 μM LDN193189 (Miltenyi Biotec, Bergisch Gladbach), and 40 μM SB-431542 (Axon Medchem). Hereafter, EBs were flushed out and transferred to a non-adherent 10 cm Petri dish (Greiner Bio-One) in differentiation medium with 500 nM smoothened agonis; SAG (Calbiochem) and 100 nM retinoic acid; and RA (Sigma-Aldrich). On day 9, 10 μM DAPT (Tocris) was added to the medium and on day 10, 20 ng/mL BDNF (Peprotech) and 10 ng/mL GDNF (Peprotech) were added. Medium was changed every other day. On day 15, EBs were dissociated into single cells using papain (Worthington Biochemical Corporation) and DNAse (Worthington Biochemical Corporation). Cells were plated on PDL (20 μg/mL, Sigma-Aldrich) and laminin (5 μg/mL, Invitrogen)-coated coverslips at 60−70% confluency.

Immunofluorescence. Cells were fixed with 4% paraformaldehyde (10 min at room temperature) and rinsed with PBS. Cells were permeabilized with 0.1% Triton X-100 (Sigma-Aldrich) and blocked with 20% goat serum in 2% BSA/PBS (45 min at room temperature). Primary antibodies were diluted in 2% FBS/0.1% Triton in PBS and incubated with the samples (overnight at 4 °C). The following primary antibodies were used: rabbit anti-tubulin-β3 (Sigma-Aldrich) and mouse anti-Isl-1 (DSHB). After a washing step with PBS, appropriate fluorescently labeled secondary antibodies (Invitrogen) were added (1 h at room temperature). Cells were then washed and mounted with Prolong Gold reagent with

DAPI (Invitrogen). The samples were imaged on a Zeiss AxioScope microscope and the images were exported and analyzed with Photoshop CS5.

Electrophysiological Recordings. We performed electrophysiological recordings on the MNs at day 25 after differentiation as described above. Individual MNs were selected for patch clamp recordings and bathed in artificial cerebrospinal fluid containing (in mM) 120 NaCl, 3.5 KCl, 1.3 MgSO$_4$, 1.25 NaH$_2$PO$_4$, 2.5 CaCl$_2$, 10 D-glucose, and 25 NaCO$_3$. We used an upright microscope (Axioskop, Zeiss) and intracellular recordings were obtained using 4–5 MΩ borosilicate glass pipettes filled with an internal solution containing (in mM) 140 K-methanesulfonate, 10 HEPES, 0.1 EGTA, 4 MgATP, and 0.3 NaGTP. Traces were collected using an Axopatch 200 amplifier (Molecular Devices), filtered with a 5 kHz filter, digitalized at 10 kHz using a Digidata 1322A (Axon Instruments, USA), and analyzed on a PC using pClamp 9.0 and Clampfit 9.2 (Axon Instruments). Recordings with a series resistance <2.5 times the pipette resistance were accepted. Cells were depolarized to induce spike trains in 10 steps of 10 nA with an interval of 30 s and a duration of 500 ms.

Proteomics. *Cell Lysis and Protein Digestion.* Samples were collected at days 0, 2, 6, 8, 10, 13, 15, 20, 22, and 24 from two healthy and two SMA biological replicates. Cells were lysed in lysis buffer containing 8 M urea in 50 mM ammonium bicarbonate (pH 8.0), one complete mini protease inhibitor (Roche), and a phosphoSTOP phosphatase inhibitor mixture (Roche). Cells were sonicated on ice and debris was removed by centrifugation at 2000g for 15 min at 4 °C. The protein concentration was determined with the Bradford assay (Bio-Rad), followed by reduction with 4 mM DTT (25 min at 56 °C) and alkylation with 8 mM iodoacetamide (30 min at room temperature in the dark). Proteins were digested into peptides using 1 μg Lys-C per 75 μg protein (4 h at 37 °C). The solution was diluted to a final urea concentration of 2 M with 50 mM ammonium bicarbonate and further digested with 1 μg trypsin per 100 μg protein (overnight at 37 °C). The digestion was quenched with 5% formic acid and peptides were desalted using Sep-Pak C18 cartridges (Waters) and vacuum centrifuged to dryness.

TMT 10-Plex Labeling. Digested aliquots of ~100 μg of each sample were chemically labeled according to the instructions outlined in the TMT reagent labeling kit (Thermo Fisher). Each label reagent tag was assigned to samples illustrated in Table S4. Peptides were resuspended in 80 μL resuspension buffer containing 50 mM HEPES buffer and 12.5% acetonitrile (ACN, pH 8.5). TMT reagents (0.8 mg) were dissolved in 80 μL anhydrous ACN of which 20 μL was added to the peptides. Following incubation at room temperature for 1 h, the reaction was then quenched using 5% hydroxylamine in HEPES buffer for 15 min at room temperature. The TMT-labeled samples were pooled with an equal protein ratio, followed by vacuum centrifugation to near dryness and desalting using Sep-Pak C18 cartridges.

Off-Line Basic pH Fractionation. Peptides were separated by basic pH reverse-phase HPLC. Samples were solubilized in buffer A (5% ACN, 10 mM ammonium bicarbonate, and pH 8.0) and subjected to a 50 min linear gradient from 18 to 45% ACN in 10 mM ammonium bicarbonate pH 8 at flow rate of 0.8 mL/min. An Agilent 1100 pump equipped with a degasser and a photodiode array detector was used with an Agilent 300 extend C18 column (5

μm particles, 4.6 mm inner diameter, and 20 cm length). The peptide mixture was then fractionated into 96 fractions and consolidated into 24 fractions. Samples were acidified with 10% formic acid and vacuum-dried, followed by redissolving with 5% formic acid/5% ACN for LC–MS/MS processing.

Mass Spectrometry Analysis. Each fraction was analyzed by nanoLC ESI MSMS using an Orbitrap Fusion (Thermo Fisher Scientific) coupled to an Agilent 1290 HPLC system (Agilent Technologies). Peptides were separated on a double frit trap column of a 20 mm × 100 μm inner diameter (ReproSil C18, Dr. Maisch GmbH, Ammerbuch, Germany). This was followed by a 40 cm × 50 μm inner diameter analytical column [ReproSil Pur C18-AQ (Dr. Maisch GmbH, Ammerbuch, Germany)]. Both columns were packed in house. Trapping was done at 5 μL/min in 0.1 M acetic acid in H$_2$O for 10 min and the analytical separation was done at 100 nL/min for 2 h by increasing the concentration of 0.1 M acetic acid in 80% acetonitrile (v/v). The instrument was operated in a data-dependent mode to automatically switch between MS and MS/MS. Full-scan MS spectra were acquired in the Orbitrap from m/z 350–1500 with a resolution of 60,000 FHMW, automatic gain control target of 400,000, and a maximum injection time of 50 ms. For the MS/MS analysis, the 10 most intense precursors at a threshold above 5000 were selected for MS/MS with an isolation width of 0.7 Th after accumulation to a target value of 30,000 (the maximum injection time was 115 ms). Fragmentation was carried out using higher-energy collisional dissociation (HCD) with a collision energy of 38% and an activation time of 0.1 ms. Fragment ion analysis was performed on Orbitrap with a resolution of 60,000 FHMW and a low mass cut-off setting of 120 m/z. Data were acquired using Xcalibur software (Thermo Scientific).

Data Processing. To process the MS raw files, we employed Proteome Discover (version 2.2, Thermo Scientific). The peak list was searched using the Swissprot database (version 2017_02) with the search engine Mascot (version 2.3, Matrix Science). Enzyme specificity was set to trypsin and allowed cleaving the N-terminal to proline up to two missed cleavages. Peptides had to have a minimum length of seven amino acids to be considered for identification. Taxonomy was chosen for *Homo sapiens* and precursor mass tolerance was set to 50 ppm with 0.05 Da fragment mass tolerance. TMT tags on lysine residues and peptide N termini (+229.163 Da) and oxidation of methionine residues (+15.995 Da) were set as dynamic modifications, while carbamidomethylation on cysteine residues (+57.021 Da) was set as static modification. For the reporter ion quantification, integration tolerance was set to 20 ppm with the most confident centroid method. The mass analyzer was done with FTMS with the MS2 order. The activation type was done with HCD with a minimum collision energy of 0 and the maximum of 1000. The results were filtered with a Mascot score of at least 20 and a percolator was used to adjust the peptide-spectrum matches to a FDR below 1%.

Bioinformatics Analysis. The open PERSEUS environment was used for statistical and bioinformatics analysis and to generate the plots and figures. For several plots, we also used GraphPad Prism (version 7.04). To compare the relative protein ratios within the samples, the values of each time point were normalized to the reference value of T1 (iPSCs) and log$_2$ transformed. All peptide ratios were then normalized against the median. To identify the most discriminating proteins

between SMA and controls, we applied a *t*-test statistics with a permutation-based FDR of 5% and S0 of 0.1 (the S0 parameter sets a threshold for the minimum fold change[78]). The significantly enriched proteins were then analyzed for annotation enrichments for GO using ShinyGO database v0.61.[79] Network analysis was performed using Cytoscape[80] with GeneMania plugin.[81]

■ ASSOCIATED CONTENT

Ⓢ Supporting Information

The Supporting Information is available free of charge at https://pubs.acs.org/doi/10.1021/acsomega.1c04688.

> Expression changes of proteins significantly altered in SMA vs. healthy MNs at indicated time points during differentiation (XLSX)

> Gene ontology analysis of the significantly enriched proteins (XLSX)

> Proteins identified and differentially expressed in the comparison study (XLSX)

> iPSC characterization and representative positive immunostainings for nuclear and surface pluripotency antigens and spontaneous differentiation toward endoderm (AFP), mesoderm (SMA), and ectoderm (TUJ1) of all lines; normal G-band karyotype of the iPSCs for healthy control and SMA lines; volcano plots illustrating differentially expressed proteins in SMA compared to healthy controls, $\log_2$ fold change plotted against the $-\log_{10} P$ value at all time points with a significant threshold p value cut-off (0.1) and a fold change >1.3, and red represents proteins upregulated in SMA and blue represents proteins downregulated in SMA; information on patient and control lines used for this study; and TMT10plex label reagents each corresponding to a day of differentiation(PDF)

■ AUTHOR INFORMATION

Corresponding Authors

Suzy Varderidou-Minasian − *Biomolecular Mass Spectrometry and Proteomics, Bijvoet Center for Biomolecular Research and Utrecht Institute for Pharmaceutical Sciences, University of Utrecht, 3584 CH Utrecht, The Netherlands; Netherlands Proteomics Center, 3584 CH Utrecht, The Netherlands;* Present Address: University Medical Centre Utrecht Center for Molecular Medicine, Universiteitsweg 100, 3584 CG, Utrecht, The Netherlands.; ⓞ orcid.org/0000-0001-7879-4291; Email: S.Varderidou-2@umcutrecht.nl

Maarten Altelaar − *Biomolecular Mass Spectrometry and Proteomics, Bijvoet Center for Biomolecular Research and Utrecht Institute for Pharmaceutical Sciences, University of Utrecht, 3584 CH Utrecht, The Netherlands; Netherlands Proteomics Center, 3584 CH Utrecht, The Netherlands;* ⓞ orcid.org/0000-0001-5093-5945; Email: m.altelaar@uu.nl

Authors

Bert M. Verheijen − *Department of Translational Neuroscience, UMC Utrecht Brain Center, University Medical Center Utrecht, Utrecht University, 3584 CG Utrecht, The Netherlands; Department of Neurology and Neurosurgery, UMC Utrecht Brain Center, University Medical Center Utrecht, Utrecht University, 3584 CX*
Utrecht, The Netherlands; Present Address: University of Southern California, Los Angeles, CA, USA

Oliver Harschnitz − *Department of Translational Neuroscience, UMC Utrecht Brain Center, University Medical Center Utrecht, Utrecht University, 3584 CG Utrecht, The Netherlands; Department of Neurology and Neurosurgery, UMC Utrecht Brain Center, University Medical Center Utrecht, Utrecht University, 3584 CX Utrecht, The Netherlands;* Present Address: The Center for Stem Cell Biology, Sloan Kettering Institute for Cancer Research, New York, USA & Developmental Biology Program, Sloan Kettering Institute for Cancer Research, New York, USA.

Sandra Kling − *Department of Translational Neuroscience, UMC Utrecht Brain Center, University Medical Center Utrecht, Utrecht University, 3584 CG Utrecht, The Netherlands; Department of Neurology and Neurosurgery, UMC Utrecht Brain Center, University Medical Center Utrecht, Utrecht University, 3584 CX Utrecht, The Netherlands*

Henk Karst − *Department of Translational Neuroscience, UMC Utrecht Brain Center, University Medical Center Utrecht, Utrecht University, 3584 CG Utrecht, The Netherlands*

W. Ludo van der Pol − *Department of Neurology and Neurosurgery, UMC Utrecht Brain Center, University Medical Center Utrecht, Utrecht University, 3584 CX Utrecht, The Netherlands*

R. Jeroen Pasterkamp − *Department of Translational Neuroscience, UMC Utrecht Brain Center, University Medical Center Utrecht, Utrecht University, 3584 CG Utrecht, The Netherlands*

Complete contact information is available at:
https://pubs.acs.org/10.1021/acsomega.1c04688

Notes

The authors declare no competing financial interest.

Data availability: All mass spectrometry proteomics data have been deposited to the ProteomeXchange Consortium via the PRIDE partner repository with the dataset identifier PXD015115. Username: reviewer26930@ebi.ac.uk. Password: pjQkMDoA.

■ ACKNOWLEDGMENTS

■ ABBREVIATIONS

iPSC, induced pluripotent stem cell; SMA, spinal muscular atrophy; SMN, survival of motor neuron; GO, Gene Ontology; TMT, tandem mass tag

■ REFERENCES

(1) Lunn, M. R.; Wang, C. H. Spinal muscular atrophy. *Lancet* **2008**, *371*, 2120−2133.

(2) Verhaart, I. E. C.; Robertson, A.; Wilson, I. J.; Aartsma-Rus, A.; Cameron, S.; Jones, C. C.; Cook, S. F.; Lochmüller, H. Prevalence, incidence and carrier frequency of 5q-linked spinal muscular atrophy - a literature review. *Orphanet J. Rare Dis.* **2017**, *12*, 124.

(3) Crawford, T. O.; Pardo, C. A. The neurobiology of childhood spinal muscular atrophy. *Neurobiol. Dis.* **1996**, *3*, 97−110.

(4) Finkel, R. S.; Mercuri, E.; Meyer, O. H.; Simonds, A. K.; Schroth, M. K.; Graham, R. J.; Kirschner, J.; Iannaccone, S. T.; Crawford, T. O.; et al. Diagnosis and management of spinal muscular atrophy: Part 2: Pulmonary and acute care; medications, supplements and immunizations; other organ systems; and ethics. *Neuromuscular Disord.* **2018**, *28*, 197−207.

(5) Mercuri, E.; Finkel, R. S.; Muntoni, F.; Wirth, B.; Montes, J.; Main, M.; Mazzone, E. S.; Vitale, M.; Snyder, B.; et al. Diagnosis and management of spinal muscular atrophy: Part 1: Recommendations for diagnosis, rehabilitation, orthopedic and nutritional care. *Neuromuscular Disord.* **2018**, *28*, 103−115.

(6) Lefebvre, S.; Bürglen, L.; Reboullet, S.; Clermont, O.; Burlet, P.; Viollet, L.; Benichou, B.; Cruaud, C.; Millasseau, P.; Zeviani, M.; et al. Identification and characterization of a spinal muscular atrophy-determining gene. *Cell* **1995**, *80*, 155−165.

(7) Lefebvre, S.; Burlet, P.; Liu, Q.; Bertrandy, S.; Clermont, O.; Munnich, A.; Dreyfuss, G.; Melki, J. Correlation between severity and SMN protein level in spinal muscular atrophy. *Nat. Genet.* **1997**, *16*, 265−269.

(8) Lorson, C. L.; Strasswimmer, J.; Yao, J.-M.; Baleja, J. D.; Hahnen, E.; Wirth, B.; Le, T.; Burghes, A. H. M.; Androphy, E. J. SMN oligomerization defect correlates with spinal muscular atrophy severity. *Nat. Genet.* **1998**, *19*, 63−66.

(9) Pellizzoni, L.; Charroux, B.; Dreyfuss, G. SMN mutants of spinal muscular atrophy patients are defective in binding to snRNP proteins. *Proc. Natl. Acad. Sci. U.S.A.* **1999**, *96*, 11167−11172.

(10) Lorson, C. L.; Hahnen, E.; Androphy, E. J.; Wirth, B. A single nucleotide in the SMN gene regulates splicing and is responsible for spinal muscular atrophy. *Proc. Natl. Acad. Sci. U.S.A.* **1999**, *96*, 6307−6311.

(11) Monani, U. R.; Lorson, C. L.; Parsons, D. W.; Prior, T. W.; Androphy, E. J.; Burghes, A. H. M.; McPherson, J. D. A Single Nucleotide Difference That Alters Splicing Patterns Distinguishes the SMA Gene SMN1 From the Copy Gene SMN2. *Hum. Mol. Genet.* **1999**, *8*, 1177−1183.

(12) Monani, U. R.; Lorson, C. L.; Parsons, D. W.; Prior, T. W.; Androphy, E. J.; Burghes, A. H.; McPherson, J. D. A single nucleotide difference that alters splicing patterns distinguishes the SMA gene SMN1 from the copy gene SMN2. *Hum. Mol. Genet.* **1999**, *8*, 1177−1183.

(13) Cho, S.; Dreyfuss, G. A degron created by SMN2 exon 7 skipping is a principal contributor to spinal muscular atrophy severity. *Genes Dev.* **2010**, *24*, 438−442.

(14) Le, T. T.; Pham, L. T.; Butchbach, M. E. R.; Zhang, H. L.; Monani, U. R.; Coovert, D. D.; Gavrilina, T. O.; Xing, L.; Bassell, G. J.; Burghes, A. H. M. SMNDelta7, the major product of the centromeric survival motor neuron (SMN2) gene, extends survival in mice with spinal muscular atrophy and associates with full-length SMN. *Hum. Mol. Genet.* **2005**, *14*, 845−857.

(15) Liu, Q.; Fischer, U.; Wang, F.; Dreyfuss, G. The spinal muscular atrophy disease gene product, SMN, and its associated protein SIP1 are in a complex with spliceosomal snRNP proteins. *Cell* **1997**, *90*, 1013−1021.

(16) Pellizzoni, L.; Kataoka, N.; Charroux, B.; Dreyfuss, G. A Novel Function for SMN, the Spinal Muscular Atrophy Disease Gene Product, in Pre-mRNA Splicing. *Cell* **1998**, *95*, 615−624.

(17) Sleigh, J. N.; Gillingwater, T. H.; Talbot, K. The contribution of mouse models to understanding the pathogenesis of spinal muscular atrophy. *Dis. Models Mech.* **2011**, *4*, 457−467.

(18) Burghes, A. H. M.; Beattie, C. E. Spinal muscular atrophy: why do low levels of survival motor neuron protein make motor neurons sick? *Nat. Rev. Neurosci.* **2009**, *10*, 597−609.

(19) Monani, U. R. Spinal muscular atrophy: a deficiency in a ubiquitous protein; a motor neuron-specific disease. *Neuron* **2005**, *48*, 885−895.

(20) Zhang, Z.; Lotti, F.; Dittmar, K.; Younis, I.; Wan, L.; Kasim, M.; Dreyfuss, G. SMN deficiency causes tissue-specific perturbations in the repertoire of snRNAs and widespread defects in splicing. *Cell* **2008**, *133*, 585−600.

(21) Bäumer, D.; Lee, S.; Nicholson, G.; Davies, J. L.; Parkinson, N. J.; Murray, L. M.; Gillingwater, T. H.; Ansorge, O.; Davies, K. E.; Talbot, K. Alternative splicing events are a late feature of pathology in a mouse model of spinal muscular atrophy. *PLoS Genet.* **2009**, *5*, No. e1000773.

(22) Fan, L.; Simard, L. R. Survival motor neuron (SMN) protein: role in neurite outgrowth and neuromuscular maturation during neuronal differentiation and development. *Hum. Mol. Genet.* **2002**, *11*, 1605−1614.

(23) Rossoll, W.; Jablonka, S.; Andreassi, C.; Kröning, A.-K.; Karle, K.; Monani, U. R.; Sendtner, M. Smn, the spinal muscular atrophy-determining gene product, modulates axon growth and localization of beta-actin mRNA in growth cones of motoneurons. *J. Cell Biol.* **2003**, *163*, 801−812.

(24) Fallini, C.; Bassell, G. J.; Rossoll, W. Spinal muscular atrophy: the role of SMN in axonal mRNA regulation. *Brain Res.* **2012**, *1462*, 81−92.

(25) Kariya, S.; Park, G.-H.; Maeno-Hikichi, Y.; Leykekhman, O.; Lutz, C.; Arkovitz, M. S.; Landmesser, L. T.; Monani, U. R. Reduced SMN protein impairs maturation of the neuromuscular junctions in mouse models of spinal muscular atrophy. *Hum. Mol. Genet.* **2008**, *17*, 2552−2569.

(26) Boyd, P. J.; Gillingwater, T. H. Chapter 8—Axonal and Neuromuscular Junction Pathology in Spinal Muscular Atrophy. In *Spinal Muscular Atrophy*; Sumner, C. J., Paushkin, S., Ko, C.-P., Eds.; Academic Press, 2017; pp 133−151.

(27) Mercuri, E.; Pera, M. C.; Scoto, M.; Finkel, R.; Muntoni, F. Spinal muscular atrophy - insights and challenges in the treatment era. *Nat. Rev. Neurol.* **2020**, *16*, 706−715.

(28) Kong, L.; Valdivia, D. O.; Simon, C. M.; Hassinan, C. W.; Delestrée, N.; Ramos, D. M.; Park, J. H.; Pilato, C. M.; Xu, X.; Crowder, M.; Grzyb, C. C.; King, Z. A.; Petrillo, M.; Swoboda, K. J.; Davis, C.; Lutz, C. M.; Stephan, A. H.; Zhao, X.; Weetall, M.; Naryshkin, N. A.; Crawford, T. O.; Mentis, G. Z.; Sumner, C. J. Impaired prenatal motor axon development necessitates early therapeutic intervention in severe SMA. *Sci. Transl. Med.* **2021**, *13*, 13.

(29) Pino, M. G.; Rich, K. A.; Kolb, S. J. Update on Biomarkers in Spinal Muscular Atrophy. *Biomarker Insights* **2021**, *16*, 11772719211035643.

(30) Takahashi, K.; Tanabe, K.; Ohnuki, M.; Narita, M.; Ichisaka, T.; Tomoda, K.; Yamanaka, S. Induction of pluripotent stem cells from adult human fibroblasts by defined factors. *Cell* **2007**, *131*, 861−872.

(31) Ebert, A. D.; Svendsen, C. N. Stem cell model of spinal muscular atrophy. *Arch. Neurol.* **2010**, *67*, 665−669.

(32) Sareen, D.; Ebert, A. D.; Heins, B. M.; McGivern, J. V.; Ornelas, L.; Svendsen, C. N. Inhibition of apoptosis blocks human motor neuron cell death in a stem cell model of spinal muscular atrophy. *PLoS One* **2012**, *7*, No. e39113.

(33) Barrett, R.; Ornelas, L.; Yeager, N.; Mandefro, B.; Sahabian, A.; Lenaeus, L.; Targan, S. R.; Svendsen, C. N.; Sareen, D. Reliable generation of induced pluripotent stem cells from human lympho-blastoid cell lines. *Stem Cells Transl. Med.* **2014**, *3*, 1429−1434.

(34) Fuller, H. R.; Mandefro, B.; Shirran, S. L.; Gross, A. R.; Kaus, A. S.; Botting, C. H.; Morris, G. E.; Sareen, D. Spinal Muscular Atrophy Patient iPSC-Derived Motor Neurons Have Reduced Expression of Proteins Important in Neuronal Development. *Front. Cell. Neurosci.* **2015**, *9*, 506.

(35) Rodriguez-Muela, N.; Litterman, N. K.; Norabuena, E. M.; Mull, J. L.; Galazo, M. J.; Sun, C.; Ng, S.-Y.; Makhortova, N. R.; White, A.; Lynes, M. M.; Chung, W. K.; Davidow, L. S.; Macklis, J. D.; Rubin, L. L. Single-Cell Analysis of SMN Reveals Its Broader Role in Neuromuscular Disease. *Cell Rep.* **2017**, *18*, 1484−1498.

(36) Ng, S.-Y.; Soh, B. S.; Rodriguez-Muela, N.; Hendrickson, D. G.; Price, F.; Rinn, J. L.; Rubin, L. L. Genome-wide RNA-Seq of Human Motor Neurons Implicates Selective ER Stress Activation in Spinal Muscular Atrophy. *Cell Stem Cell* **2015**, *17*, 569−584.

(37) Varderidou-Minasian, S.; Verheijen, B. M.; Schätzle, P.; Hoogenraad, C. C.; Pasterkamp, R. J.; Altelaar, M. Deciphering the Proteome Dynamics during Development of Neurons Derived from Induced Pluripotent Stem Cells. *J. Proteome Res.* **2020**, *19*, 2391−2403.

(38) Lindhout, F. W.; Kooistra, R.; Portegies, S.; Herstel, L. J.; Stucchi, R.; Snoek, B. L.; Altelaar, A. M.; MacGillavry, H. D.; Wierenga, C. J.; Hoogenraad, C. C. Quantitative mapping of transcriptome and proteome dynamics during polarization of human iPSC-derived neurons. *Elife* **2020**, *9*, No. e58124.

(39) Varderidou-Minasian, S.; Hinz, L.; Hagemans, D.; Posthuma, D.; Altelaar, M.; Heine, V. M. Quantitative proteomic analysis of Rett iPSC-derived neuronal progenitors. *Mol. Autism* **2020**, *11*, 38.

(40) Rademacher, S.; Verheijen, B. M.; Hensel, N.; Peters, M.; Bora, G.; Brandes, G.; Vieira de Sá, R.; Heidrich, N.; Fischer, S.; Brinkmann, H.; van der Pol, W. L.; Wirth, B.; Pasterkamp, R. J.; Claus, P. Metalloprotease-mediated cleavage of PlexinD1 and its sequestration to actin rods in the motoneuron disease spinal muscular atrophy (SMA). *Hum. Mol. Genet.* **2017**, *26*, 3946−3959.

(41) Harschnitz, O.; van den Berg, L. H.; Johansen, L. E.; Jansen, M. D.; Kling, S.; Vieira de Sá, R.; Vlam, L.; van Rheenen, W.; Karst, H.; Wierenga, C. J.; Pasterkamp, R. J.; van der Pol, W. L. Autoantibody pathogenicity in a multifocal motor neuropathy induced pluripotent stem cell-derived model. *Ann. Neurol.* **2016**, *80*, 71−88.

(42) Maury, Y.; Côme, J.; Piskorowski, R. A.; Salah-Mohellibi, N.; Chevaleyre, V.; Peschanski, M.; Martinat, C.; Nedelec, S. Combinatorial analysis of developmental cues efficiently converts human pluripotent stem cells into multiple neuronal subtypes. *Nat. Biotechnol.* **2014**, *33*, 89.

(43) Chambers, S. M.; Fasano, C. A.; Papapetrou, E. P.; Tomishima, M.; Sadelain, M.; Studer, L. Highly efficient neural conversion of human ES and iPS cells by dual inhibition of SMAD signaling. *Nat. Biotechnol.* **2009**, *27*, 275−280.

(44) Fuller, H. R.; Man, N. T.; Lam, L. T.; Shamanin, V. A.; Androphy, E. J.; Morris, G. E. Valproate and bone loss: iTRAQ proteomics show that valproate reduces collagens and osteonectin in SMA cells. *J. Proteome Res.* **2010**, *9*, 4228−4233.

(45) Chaves-Filho, A. B.; Pinto, I. F. D.; Dantas, L. S.; Xavier, A. M.; Inague, A.; Faria, R. L.; Medeiros, M. H. G.; Glezer, I.; Yoshinaga, M. Y.; Miyamoto, S. Alterations in lipid metabolism of spinal cord linked to amyotrophic lateral sclerosis. *Sci. Rep.* **2019**, *9*, 11642.

(46) Li, H.; Custer, S. K.; Gilson, T.; Hao, L. T.; Beattie, C. E.; Androphy, E. J. alpha-COP binding to the survival motor neuron protein SMN is required for neuronal process outgrowth. *Hum. Mol. Genet.* **2015**, *24*, 7295−7307.

(47) Powis, R. A.; Karyka, E.; Boyd, P.; Come, J.; Jones, R. A.; Zheng, Y.; Szunyogova, E.; Groen, E. J.; Hunter, G.; Thomson, D.; Wishart, T. M.; Becker, C. G.; Parson, S. H.; Martinat, C.; Azzouz, M.; Gillingwater, T. H. Systemic restoration of UBA1 ameliorates disease in spinal muscular atrophy. *JCI Insight* **2016**, *1*, No. e87908.

(48) Borg, R.; Cauchi, R. J. The Gemin associates of survival motor neuron are required for motor function in Drosophila. *PLoS One* **2013**, *8*, No. e83878.

(49) Thompson, L. W.; Morrison, K. D.; Shirran, S. L.; Groen, E. J. N.; Gillingwater, T. H.; Botting, C. H.; Sleeman, J. E. Neurochondrin interacts with the SMN protein suggesting a novel mechanism for spinal muscular atrophy pathology. *J. Cell Sci.* **2018**, *131*, jcs211482.

(50) Haramati, S.; Chapnik, E.; Sztainberg, Y.; Eilam, R.; Zwang, R.; Gershoni, N.; McGlinn, E.; Heiser, P. W.; Wills, A.-M.; Wirguin, I.; Rubin, L. L.; Misawa, H.; Tabin, C. J.; Brown, R., Jr.; Chen, A.;

Hornstein, E. miRNA malfunction causes spinal motor neuron disease. *Proc. Natl. Acad. Sci. U.S.A.* **2010**, *107*, 13111−13116.

(51) Rossoll, W.; Kröning, A.-K.; Ohndorf, U.-M.; Steegborn, C.; Jablonka, S.; Sendtner, M. Specific interaction of Smn, the spinal muscular atrophy determining gene product, with hnRNP-R and gry-rbp/hnRNP-Q: a role for Smn in RNA processing in motor axons? *Hum. Mol. Genet.* **2002**, *11*, 93−105.

(52) Mourelatos, Z.; Abel, L.; Yong, J.; Kataoka, N.; Dreyfuss, G. SMN interacts with a novel family of hnRNP and spliceosomal proteins. *EMBO J.* **2001**, *20*, 5443−5452.

(53) Wu, C.-H.; Fallini, C.; Ticozzi, N.; Keagle, P. J.; Sapp, P. C.; Piotrowska, K.; Lowe, P.; Koppers, M.; McKenna-Yasek, D.; et al. Mutations in the profilin 1 gene cause familial amyotrophic lateral sclerosis. *Nature* **2012**, *488*, 499−503.

(54) Motyl, A. A. L.; Faller, K. M. E.; Groen, E. J. N.; Kline, R. A.; Eaton, S. L.; Ledahawsky, L. M.; Chaytow, H.; Lamont, D. J.; Wishart, T. M.; Huang, Y.-T.; Gillingwater, T. H. Pre-natal manifestation of systemic developmental abnormalities in spinal muscular atrophy. *Hum. Mol. Genet.* **2020**, *29*, 2674−2683.

(55) Finkel, R. S.; Crawford, T. O.; Swoboda, K. J.; Kaufmann, P.; Juhasz, P.; Li, X.; Guo, Y.; Li, R. H.; Trachtenberg, F.; Forrest, S. J.; Kobayashi, D. T.; Chen, K. S.; Joyce, C. L.; Plasterer, T. Candidate proteins, metabolites and transcripts in the Biomarkers for Spinal Muscular Atrophy (BforSMA) clinical study. *PLoS One* **2012**, *7*, No. e35462.

(56) Fuller, H. R.; Mandefro, B.; Shirran, S. L.; Gross, A. R.; Kaus, A. S.; Botting, C. H.; Morris, G. E.; Sareen, D. Spinal Muscular Atrophy Patient iPSC-Derived Motor Neurons Have Reduced Expression of Proteins Important in Neuronal Development. *Front. Cell. Neurosci.* **2016**, *9*, 506.

(57) Groen, E. J. N.; Talbot, K.; Gillingwater, T. H. Advances in therapy for spinal muscular atrophy: promises and challenges. *Nat. Rev. Neurol.* **2018**, *14*, 214−224.

(58) Peter, C. J.; Evans, M.; Thayanithy, V.; Taniguchi-Ishigaki, N.; Bach, I.; Kolpak, A.; Bassell, G. J.; Rossoll, W.; Lorson, C. L.; Bao, Z.-Z.; Androphy, E. J. The COPI vesicle complex binds and moves with survival motor neuron within axons. *Hum. Mol. Genet.* **2011**, *20*, 1701−1711.

(59) Ng, S.-Y.; Soh, B. S.; Rodriguez-Muela, N.; Hendrickson, D. G.; Price, F.; Rinn, J. L.; Rubin, L. L. Genome-wide RNA-Seq of Human Motor Neurons Implicates Selective ER Stress Activation in Spinal Muscular Atrophy. *Cell Stem Cell* **2015**, *17*, 569−584.

(60) Pellizzoni, L.; Yong, J.; Dreyfuss, G. Essential role for the SMN complex in the specificity of snRNP assembly. *Science* **2002**, *298*, 1775−1779.

(61) Altelaar, A. F. M.; Frese, C. K.; Preisinger, C.; Hennrich, M. L.; Schram, A. W.; Timmers, H. T. M.; Heck, A. J. R.; Mohammed, S. Benchmarking stable isotope labeling based quantitative proteomics. *J. Proteom.* **2013**, *88*, 14−26.

(62) Boza-Morán, M. G.; Martínez-Hernández, R.; Bernal, S.; Wanisch, K.; Also-Rallo, E.; Le Heron, A.; Alías, L.; Denis, C.; Girard, M.; Yee, J.-K.; Tizzano, E. F.; Yáñez-Muñoz, R. J. Decay in survival motor neuron and plastin 3 levels during differentiation of iPSC-derived human motor neurons. *Sci. Rep.* **2015**, *5*, 11696.

(63) Groen, E. J. N.; Perenthaler, E.; Courtney, N. L.; Jordan, C. Y.; Shorrock, H. K.; van der Hoorn, D.; Huang, Y.-T.; Murray, L. M.; Viero, G.; Gillingwater, T. H. Temporal and tissue-specific variability of SMN protein levels in mouse models of spinal muscular atrophy. *Hum. Mol. Genet.* **2018**, *27*, 2851−2862.

(64) Rossoll, W.; Jablonka, S.; Andreassi, C.; Kroning, A.-K.; Karle, K.; Monani, U. R.; Sendtner, M. Smn, the spinal muscular atrophy-determining gene product, modulates axon growth and localization of beta-actin mRNA in growth cones of motoneurons. *J. Cell Biol.* **2003**, *163*, 801−812.

(65) Carrel, T. L.; McWhorter, M. L.; Workman, E.; Zhang, H.; Wolstencroft, E. C.; Lorson, C.; Bassell, G. J.; Burghes, A. H. M.; Beattie, C. E. Survival motor neuron function in motor axons is independent of functions required for small nuclear ribonucleoprotein biogenesis. *J. Neurosci.* **2006**, *26*, 11014−11022.

(66) Cauchi, R. J. SMN and Gemins: 'we are family' ... or are we?: insights into the partnership between Gemins and the spinal muscular atrophy disease protein SMN. *Bioessays* **2010**, *32*, 1077−1089.

(67) Naryshkin, N. A.; Weetall, M.; Dakka, A.; Narasimhan, J.; Zhao, X.; Feng, Z.; Ling, K. K. Y.; Karp, G. M.; Qi, H.; Woll, M. G.; Chen, G.; Zhang, N.; et al. Motor neuron disease. SMN2 splicing modifiers improve motor function and longevity in mice with spinal muscular atrophy. *Science* **2014**, *345*, 688−693.

(68) Soucy, T. A.; Smith, P. G.; Milhollen, M. A.; Berger, A. J.; Gavin, J. M.; Adhikari, S.; Brownell, J. E.; Burke, K. E.; Cardin, D. P.; et al. An inhibitor of NEDD8-activating enzyme as a new approach to treat cancer. *Nature* **2009**, *458*, 732−736.

(69) Emanuele, M. J.; Elia, A. E. H.; Xu, Q.; Thoma, C. R.; Izhar, L.; Leng, Y.; Guo, A.; Chen, Y.-N.; Rush, J.; Hsu, P. W.-C.; Yen, H.-C. S.; Elledge, S. J. Global identification of modular cullin-RING ligase substrates. *Cell* **2011**, *147*, 459−474.

(70) Schwartz, W. J.; Klerman, E. B. Circadian Neurobiology and the Physiologic Regulation of Sleep and Wakefulness. *Neurol. Clin.* **2019**, *37*, 475−486.

(71) Adriaenssens, E.; Geuens, T.; Baets, J.; Echaniz-Laguna, A.; Timmerman, V. Novel insights in the disease biology of mutant small heat shock proteins in neuromuscular diseases. *Brain* **2017**, *140*, 2541−2549.

(72) Taylor, A. S.; Glascock, J. J.; Rose, F. F., Jr.; Lutz, C.; Lorson, C. L. Restoration of SMN to Emx-1 expressing cortical neurons is not sufficient to provide benefit to a severe mouse model of Spinal Muscular Atrophy. *Transgenic Res.* **2013**, *22*, 1029−1036.

(73) Wishart, T. M.; Huang, J. P.-W.; Murray, L. M.; Lamont, D. J.; Mutsaers, C. A.; Ross, J.; Geldsetzer, P.; Ansorge, O.; Talbot, K.; Parson, S. H.; Gillingwater, T. H. SMN deficiency disrupts brain development in a mouse model of severe spinal muscular atrophy. *Hum. Mol. Genet.* **2010**, *19*, 4216−4228.

(74) Sances, S.; Ho, R.; Vatine, G.; West, D.; Laperle, A.; Meyer, A.; Godoy, M.; Kay, P. S.; Mandefro, B.; Hatata, S.; Hinojosa, C.; Wen, N.; Sareen, D.; Hamilton, G. A.; Svendsen, C. N. Human iPSC-Derived Endothelial Cells and Microengineered Organ-Chip Enhance Neuronal Development. *Stem Cell Rep.* **2018**, *10*, 1222−1236.

(75) Osaki, T.; Uzel, S. G. M.; Kamm, R. D. Microphysiological 3D model of amyotrophic lateral sclerosis (ALS) from human iPS-derived muscle cells and optogenetic motor neurons. *Sci. Adv.* **2018**, *4*, No. eaat5847.

(76) Warlich, E.; Kuehle, J.; Cantz, T.; Brugman, M. H.; Maetzig, T.; Galla, M.; Filipczyk, A. A.; Halle, S.; Klump, H.; Schöler, H. R.; Baum, C.; Schroeder, T.; Schambach, A. Lentiviral vector design and imaging approaches to visualize the early stages of cellular reprogramming. *Mol. Ther.* **2011**, *19*, 782−789.
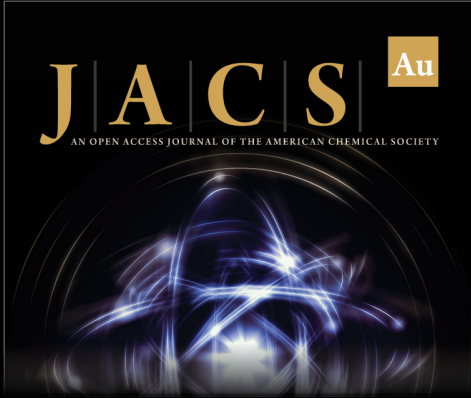
(77) Rivron, N. C.; Vrij, E. J.; Rouwkema, J.; Le Gac, S.; van den Berg, A.; Truckenmuller, R. K.; van Blitterswijk, C. A. Tissue deformation spatially modulates VEGF signaling and angiogenesis. *Proc. Natl. Acad. Sci. U.S.A.* **2012**, *109*, 6886−6891.

(78) Tusher, V. G.; Tibshirani, R.; Chu, G. Significance analysis of microarrays applied to the ionizing radiation response. *Proc. Natl. Acad. Sci. U.S.A.* **2001**, *98*, 5116−5121.

(79) Ge, S. X.; Jung, D.; Yao, R. ShinyGO: a graphical enrichment tool for animals and plants. *Bioinformatics* **2020**, *36*, 2628−2629.

(80) Shannon, P.; Markiel, A.; Ozier, O.; Baliga, N. S.; Wang, J. T.; Ramage, D.; Amin, N.; Schwikowski, B.; Ideker, T. Cytoscape: a software environment for integrated models of biomolecular interaction networks. *Genome Res.* **2003**, *13*, 2498−2504.

(81) Montojo, J.; Zuberi, K.; Rodriguez, H.; Kazi, F.; Wright, G.; Donaldson, S. L.; Morris, Q.; Bader, G. D. GeneMANIA Cytoscape plugin: fast gene function predictions on the desktop. *Bioinformatics* **2010**, *26*, 2927−2928.